Engineering and Technology Journal
Journal homepage: https://etj.uotechnology.edu.iq

Evaluation of the Performance of Steel Slag and Waste Glass as a Cement Replacement

Ahmed T. Azeez[a*], **Maan S. Hassan**[b], **Alaa A. Atiyah**[a]

[a] Material Engineering Dept., University of Technology-Iraq, Alsina'a street, 10066 Baghdad, Iraq.
[b] Civil Engineering Dept., University of Technology-Iraq, Alsina'a street, 10066 Baghdad, Iraq.
*Corresponding author Email: ahmad.taifor@koyauniversity.org

HIGHLIGHTS

- This work assessed the pozzolanic activity of locally available steel slag and waste glass in mortars.
- Effects of steel slag and waste glass replacing cement on workability, density, and strength index are studied.
- Unlike waste glass, steel slag decreased mortar strength and workability.
- Steel slag improved compressive strength and mitigated the negative impact of waste glass in concrete.

ARTICLE INFO

Handling editor: Akram R. Jabur

Keywords:

Concrete; Recycling; Steel slag; Strength activity index; Waste glass.

ABSTRACT

The industrial development and growth in population activity caused an annual increase in solid wastes over the past decades. The emissions of CO_2 from the cement industry are the main source of air pollution. Recycling wastes as cementitious materials conserve the ecosystem in different aspects, e.g., reduction of CO_2 footprint. Consequently, the pozzolanic activity of two solid wastes abundantly available in Iraq, steel slag (SS) and waste glass (WG), were evaluated. This study aimed to replace them with ordinary Portland cement. This will achieve a sustainable, eco-efficient, and environmentally friendly construction industry. The Chemical analysis of the wastes by XRF and XRD suggests a possible cementitious capability owing to the amorphous nature of WG and the presence of C_3S and C_2S in SS. Accordingly, due to international standards, cubic mortars were produced by replacing cement with SS at 50% and WG at 50% and 20%. The effects of such replacements on the compressive strength of mortars were evaluated by comparison with that of the control mortars. WG increases workability and results in a higher strength index (72.8%) than that of SS (48.7%) at similar replacement levels (50%). Subsequently, SS and WG replaced coarse aggregates (CA) and cement, respectively, in concrete. The results revealed positive effects of SS on compressive strength in contrast to WG influence. The compressive strength of concrete cured for 91d increased by about 20% compared to the control sample upon incorporation of 50% SS without any WG.

1. Introduction

Pollution of the environment is a significant global concern that poses serious threats to ecosystems, human health, and the planet's overall well-being. The cement industry is one of the major sources of pollution due to carbon dioxide (CO_2) emissions due to the energy-intensive nature of cement production. The trend of gas emissions is evaluated as a tonne of CO_2 per tonne of cement produced [1–3]. On the other hand, electric arc furnace steel slag (EAFS, abbreviated here as SS) and waste glass (WG) are the main by-products of human industrial activities. These wastes mostly end up in landfills, causing serious environmental issues. Contamination of agricultural fields and spring water are associated risks of SS and WG [4–6]. Accordingly, it is essential to incentivize industries to incorporate these wastes into construction materials and preferably replace cement [7]. The strategy can contribute to more sustainable building practices in addition to essential economic advantages by reducing the cost of construction materials through utilizing lower-cost wastes.

The literature considered the cementitious capability of the SS and WG intensively. However, the hydraulic activity of the SS cannot be standardized globally. SS compositions differ from plant to plant because the composition of SS relies on the judgment of engineers and workers in the field while controlling the chemistry of the molten steel [8–10]. Nevertheless, the SS may contain cementitious phases such as C_3S and β-C_2S which enable it to amend the cement. However, because SS is formed at temperature 1650 ℃ which is higher than that for cement production, the crystal structures of C_3S and β-C_2S are compacted. Consequently, they have slower hydration rates than their corresponding phases in cement [11]. Furthermore, during slow

http://doi.org/10.30684/etj.2023.143602.1597
Received 26 September 2023; Received in revised form 03 November 2023; Accepted 04 November 2023; Available online 06 December 2023
2412-0758/University of Technology-Iraq, Baghdad, Iraq

cooling, the active β-C_2S may convert to less active γ-C_2S, which is another factor for slow hydration [12]. In concrete, Osman et al. (2021) reviewed the literature to evaluate SS performance as a construction material. The bottom line of the review is that SS cannot entirely replace cement, and an optimum replacement ratio should be determined by evaluating concrete's durability and mechanical properties [13].

In contrast, WG is amorphous and siliceous and is a candidate cementitious material owing to its pozzolanic activity [14]. The silica in the glass may dissolve in the presence of an alkaline, namely portlandite $Ca(OH)_2$, to form calcium-silicate hydrates (CSH). However, to increase the pozzolanic rate, it is essential to grind the WG to small sizes, preferably below 150 μm [15]. Replacing the WG with cement brings significant benefits. For example, better mechanical properties and durability due to the reduction of the porosity content emerged from the pozzolanic reaction with portlandite [16,17]. Nevertheless, the disadvantageous effects of WG have also been reported in the literature owing to its brittleness and poor geometry [18]. This study aims to utilize locally available wastes, namely SS, which is the residue of the steel melting process of the steel plant. However, it is essential to characterize SS in advance to determine its role in the construction materials, such as cementitious or aggregates, because its chemistry largely determines its properties, which can vary depending on the production protocol in each plant. This study aims to address its cementitious capability because no contribution is observed in this direction. The research article was integrated by comparing the strength activity of SS with another waste (WG) at equal fractions of replacements. This study will provide a complete assessment of the efficiency of SS hydraulic activity with respect to ordinary Portland cement (OPC) and WG, which is approved in the literature as a pozzolanic material. In the second phase, SS will replace coarse aggregate (CA) in concrete to evaluate its performance on the compressive strength of concrete.

The SS and WG were gathered from landfills and prepared as per the standards requirement. The wastes' chemical compositions and mineralogical contents were thoroughly analyzed using XRF and XRD. The density, flowability, strength index, slump, and compressive strength were determined per the standards. The findings will evaluate the performance of SS and WG as cement replacements in mortars and SS as aggregate in concrete.

2. Methods

2.1 Materials

2.1.1 Cement

Ordinary Portland Cement (OPC) type I (42.5R) was used in this study. The cement's chemical composition and physical properties as per ASTM C150, are shown in Tables 1 and 2 [19].

2.1.2 Waste glass

The chemical composition of WG prepared in this study, as described later, was determined using XRF. The chemical requirements for the pozzolanic activity of WG were evaluated according to ASTM C618 and are shown in Table 3 [20].

2.1.3 Sand and steel slag

Natural river sand with gradation as per ASTM C33 was used. The finesse modulus and specific gravity were determined according to ASTM C128 [21], and their values were 2.82 and 2.73, respectively. On the other hand, the Hend steel plant/Erbil supplied SS, and only those particles that passed 75µm sieve were used. The chemical composition of SS is shown in Table 4 as per ASTM C989 [22]. The specific gravity of SS, according to ASTM C127, is 3.36 [23]. Moreover, SS is well known for its irregular texture and porous nature when replacing CA, see Figure 1.

2.2 Waste Glass Preparation

The residue of clear glass processing was gathered from the industrial sector in Erbil. The crushed glass was converted to a fine powder of size below 75µm in a multistep process, as shown in Figure 2.

Table 1: Chemical composition of OPC

Chemical composition	Chemical formula	OPC %	ASTM C150
Lime	CaO	64.12	
Silica	SiO_2	22.05	
Alumina	Al_2O_3	4.89	
Ferrite	Fe_2O_3	2.32	
Magnesia	MgO	4.10	≤6%
Sulfur oxide	SO_3	0.581	≤3%
Potassium oxide	K_2O	0.60	
Sodium oxide	Na_2O	0.19	
Tricalcium silicate	C_3S		55.62
Dicalcium silicate	C_2S		21.25
Tricalcium Aluminate	C_3A		9.03
Tetracalcium aluminate ferrite	C_4AF		7.06
Sodium equivalent (%)	$Na_2O+0.685K_2O$	0.601	≥ 0.6[a]

[a] requirements of ASTM C989

Table 2: Physical properties of OPC

Test	Cement	ASTM C150
Initial setting (min)	130	≥ 45
Final setting (min)	205	≤ 375
Compressive strength 7 days (MPa)	24.5	19
Compressive strength 28 days (Mpa)	45.6	-

Table 3: Chemical composition of WG

Chemical composition	Chemical formula	WG %	ASTM C618
Lime	CaO	10.50	
Silica	SiO_2	76.78	
Alumina	Al_2O_3	1.713	
Ferrite	Fe_2O_3	1.078	
Magnesia	MgO	1.146	
Sulfur oxide	SO_3	1.926	≤ 4%
Potassium oxide	K_2O	0.1	
Sodium oxide	Na_2O	7.73	
SiO_2+ Al_2O_3+ Fe_2O_3		79.57	≥ 70%

Table 4: Chemical composition of SS

Chemical composition	Chemical formula	SS %	ASTM C989
Lime	CaO	26.34	
Silica	SiO_2	10.70	
Alumina	Al_2O_3	2.40	
Ferrite	Fe_2O_3	39.26	
Magnesia	MgO	0.41	
Sulfur oxide	SO_3	2.50	≤ 3%
Potassium oxide	K_2O	1.03	
Sodium oxide	Na_2O	0.023	
Phosphorous oxide	P_2O_5	0.23	

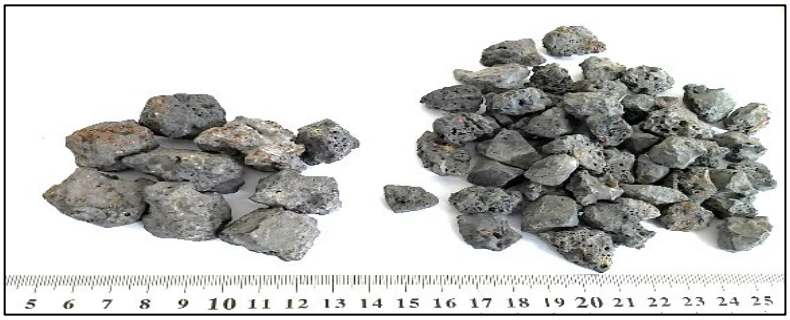

Figure 1: SS retained on sieves a) 19 mm b) 12.5 mm

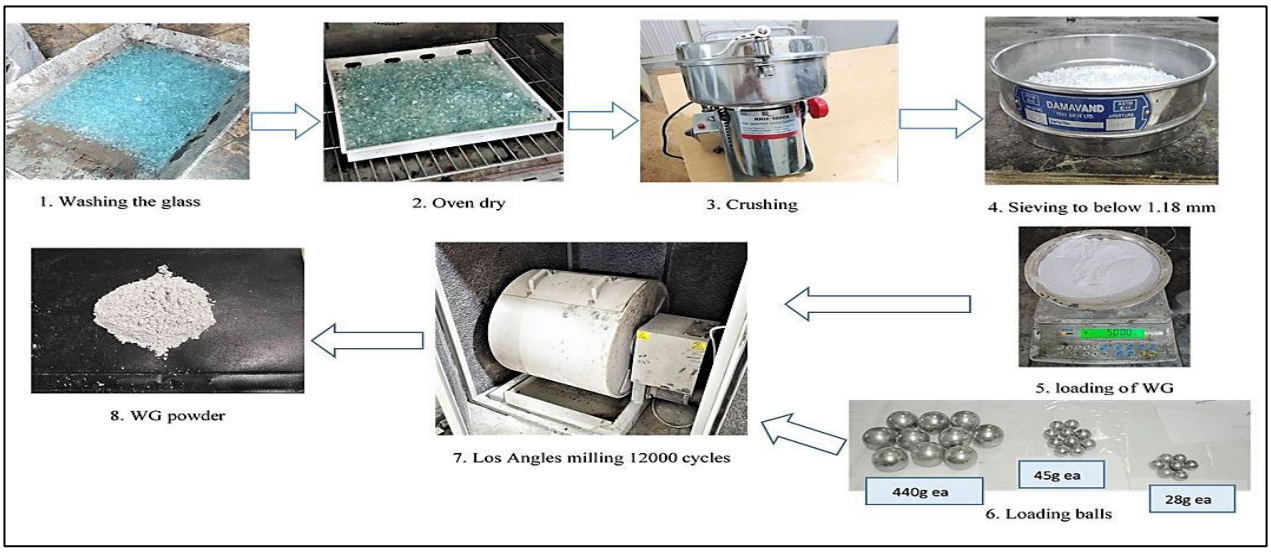

Figure 2: Preparation of the WG powder using mechanical methods

2.3 X-ray Diffraction

The phases of SS and WG crystallinity were evaluated by XRD analysis. A 6000 Shimadzu machine was used under the following measurement conditions: the x-ray tube is copper, 40 kV, 30 mA, and the scanning speed was 10 deg/min.

2.4 Sample Preparation

Mixing of the constituents was guided by ASTM C305 [24]. The mortars' casting, compacting, and curing were performed under ASTM C109 control [25]. Bottled water was used to mix the ingredients with a w/b ratio of 0.485. On the other hand, the cement: sand ratio was 1:2.75. Four samples were prepared: S1 and S3 for WG and SS, replacing cement at 20% and 50% to satisfy the ASTM C618 and ASTM C989 requirements, respectively. An additional sample, S2 (WG=50%), was prepared to compare the effects of WG on the fresh and hardened properties of the mortar with S3, in which SS replaces cement by 50% Figures 3 and 4.

2.5 Density

The saturated density of mortars upon cement replacement with SS and WG was evaluated according to ASTM C642, which is a specification for WG's chemical and physical requirements as pozzolans [26]. The cubes were removed from the water after 28 d curing. Then, the cube surfaces were dried, and their weights were divided by the volume.

2.6 Flow Table Test

Flow table test conforming to ASTM C1437 determined the effects of SS and WG on mortars' workability [27,28]. Oven-dried graded standard sand as per ASTM C778 was used [29]. Several trials were conducted to determine the w/b ratio that achieves flow within (105%-115%) as a target range.

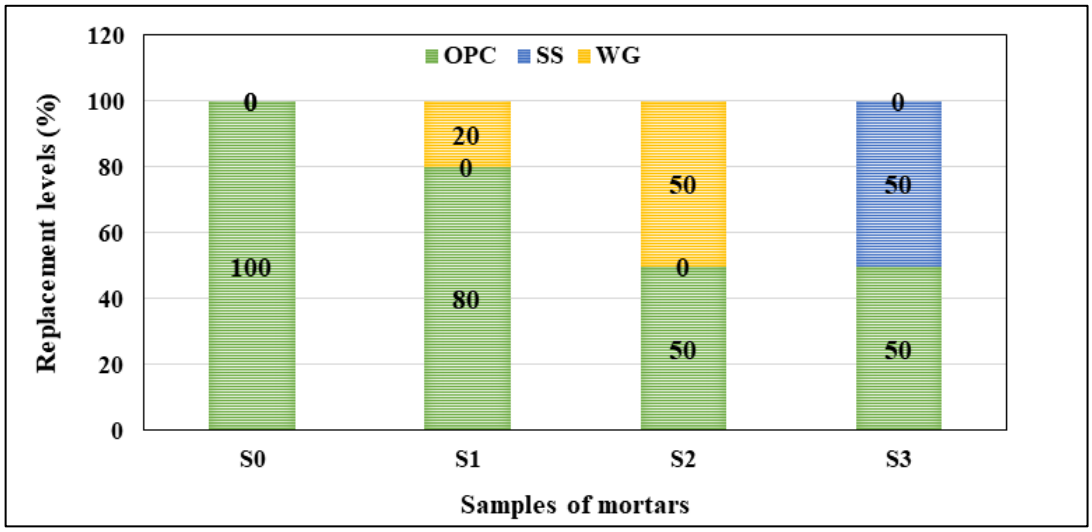

Figure 3: Mortar types S0, S1, S2, and S3

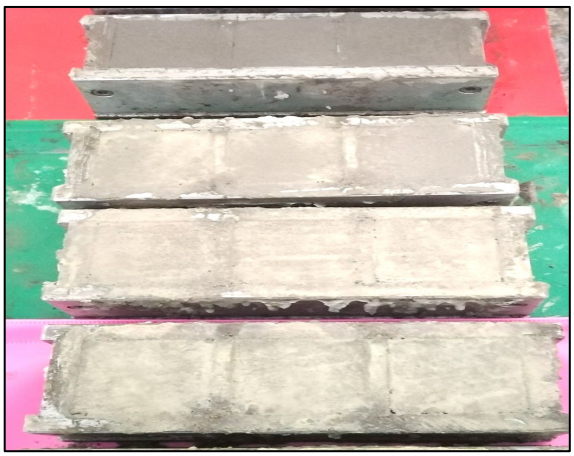

Figure 4: Casting of mortar samples the pink S0, the green S1 and S2, and the red S3

2.7 Compressive Strength of Mortars

The compressive tests were conducted according to ASTM C109, where two groups (7d and 28d curing) were investigated to satisfy the requirements of ASTM C989 and ASTM C618 [22]. A control machine was used to break the samples at a loading rate of 1500 N/s.

2.8 Steel Slag as Coarse Aggregates in Concrete

The strength index of SS and WG determines their performance in replacing the concrete constituents (cement or aggregates). The results of the strength index (discussed later) assigned SS and WG as CA and cement replacement, respectively. Accordingly, SS and WG replaced CA and cement at 50% and 15% weight, respectively. The SS aggregates were replaced with CA of corresponding sizes determined through sieve analysis. It is worth noting that only those retained on sieves 19 mm and 12.5 mm were replaced with CA see Table 5. Aggregates of size 9.5 mm and 4.75 mm were always natural and maintained constant in all samples at 153 $kg/m^3$and 51 kg/m^3, respectively.

Volume stability of SS as a CA is a serious concern because of the presence of hydraulic oxides named CaO and MgO. Accordingly, SS aged under environmental conditions for more than three months to stabilize it. Moreover, the aging process was accelerated by spraying the SS aggregates with water [30].

The concrete mix design was under the guidance of ACI 211.1 [31]. The water and sand content maintained constant throughout the trials at 170kg/m^3 and 750kg/m^3 respectively. Three cubes of dimension 100 mm were prepared per curing age (28d and 91d). The sample preparation and curing followed ASTM C192, see Figure 5 [32].

Superplasticizers (SP) were used to control the mixtures' slump within a range of 185 ∓ 25 mm to satisfy the market demand for consistent concrete to facilitate pumping. ASTM C143 and ASTM C39 controlled the slump and compressive strength, respectively [33,34]. Polycarboxylate-based superplasticizers conformed to type F of ASTM C494 standard were used with PH, density, alkali, and total chlorine of 7, 1.12 kg/L, and less than 5%, and 0.1%, respectively.

2.9 Scanning Electron Microscope (SEM)

The fracture surfaces of the samples were sliced into small pieces using an angle grinding machine. The samples were oven-dried at $110℃ \pm 5℃$ for 24 hours. The slices were gold coated to avoid surface charging under the electron beam. A machine of type Quanta 450 was used to scan the fractured surfaces.

Table 5: Proportion of mixture components (kg/m^3)

Samples	Cement	WG	19mm aggregate		12.5mm aggregate	
			SS	CA	SS	CA
A0	425	-	-	51	-	765
A1	361	64	-	51	-	765
A2	361	64	25.5	25.5	382.5	382.5
A3	425	-	25.5	25.5	382.5	382.5

Figure 5: Casting and consolidation of concrete cubes

3. Results and Discussion

3.1 X-ray Diffraction

Figure 6 shows the spectrums of XRD analysis of SS and WG. A broad peak is observed in Figure 6a, a sign of WG's amorphous nature since no sharp individual peaks (the identity of the crystalline phase) were observed. This probably suggests WG is a pozzolan material since the amorphous phases are well known for forming a net of bonds acting as an adhesive in structures [35]. On the other hand, the presence of C_3S and C_2S in the spectrum of SS Figure 6b may address it as cementitious materials. However, the hydraulic activity of SS and WG is a matter of their strength index, as discussed in the upcoming sections. The XRD spectrums of WG and SS were interpreted with respect to the references [36,37].

3.2 Density

Figure 7 shows the saturated densities of S0, S1, S2, and S3 mortars. Mortar density is a function of its ingredients' density. Accordingly, incorporating SS (S3) increased the density by about 1.4% compared to the control sample (with no substitutions). The high specific gravity of the SS compared with cement addresses the reason for increasing mortar's density upon SS incorporation. The same behavior was reported in the literature when a blend of SS and WG replaced cement. In the blends, SS counteracted the WG effect on the density as it constantly increased with SS incorporation because of its spontaneous high density due to the presence of some metals [12]. On the other hand, the WG decreased the density by about 0.6% and 1.28% at 20% and 50% replacement, respectively. Moreover, a comparison of the density of the mortars at 50% replacement for each of SS and WG (S2 and S3) makes it obvious that the former density is 2.55% higher than the latter. This is also attributed to the spontaneous high density of SS compared to WG of specific gravity of 2.55 [38].

3.3 Flow table

Table 6 lists the w/b and the corresponding flow obtained, noting that oven-dried standard-graded sand was used. WG increases mortar workability from 109% to 114% on the flow table. This increase in workability corresponds to the increase in WG replacement fraction from 20% to 50% at the same w/b ratio of 0.725. However, the control sample needed w/b=0.775 to achieve 106% flowability in mortar. The positive contribution of WG to the mortar's flowability is mainly attributed to its hydrophobicity, which retains some water, thus increasing the workability of the mortar. A similar verification was reported in the literature when concrete, regardless of its grade (45MPa or 33MPa), constantly increased the slump upon WG percentage increment when replaced with cement [39].

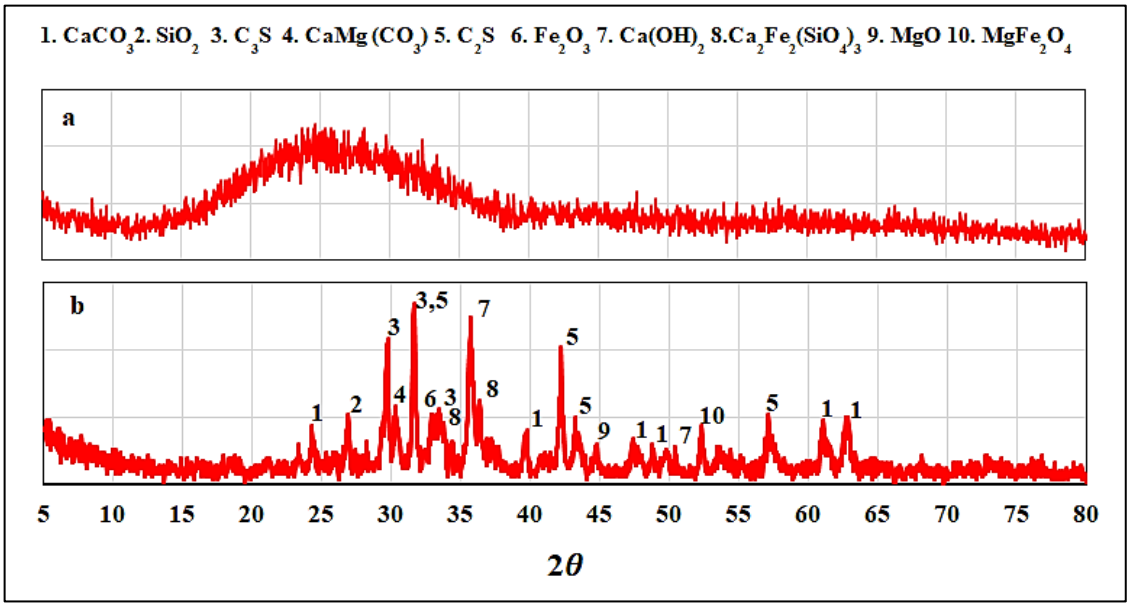

Figure 6: Results of XRD analysis a) WG b) SS

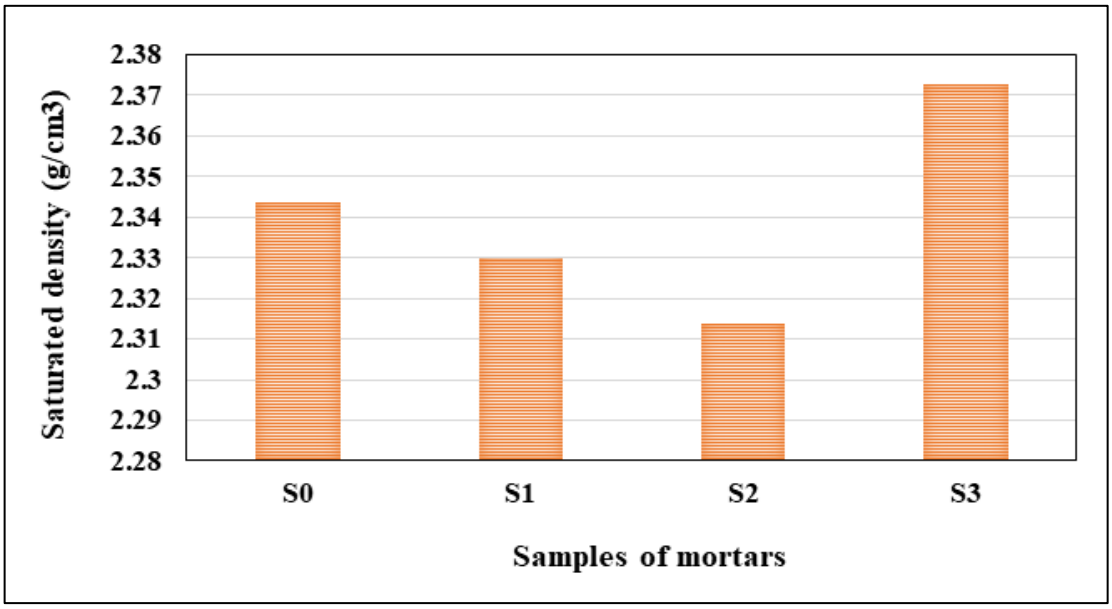

Figure 7: Saturated density of mortars S0, S1, S2, and S3

On the other hand, amending cement with WG increases the alkalinity of the mixtures owing to the higher Na_2O content than cement. See Tables 1 and 3. In the same context, Abellan et al. observed the positive effect of WG on a concrete's flow table, attributing it to its alkalinity. The increased alkalinity reduced the shear strength of the paste, increasing, in turn, the workability [38].

Regarding SS, a higher w/b (0.800) is required to achieve workability within the target range (105%-110%). This may be due to its irregular and flaky, rheologically undesirable shapes. Baalamurugan et al. also observed the heterogeneous surface texture of SS through SEM analysis. An increased demand for water by SS particles at a similar substitution level for cement as WG (20%) to achieve a comparable workability was also reported by Dawood et al. SS's irregular surface texture is believed to exert frictional forces against the paste flow, reducing its workability [12].

3.4 Compressive Strength of Mortars

Figure 8 depicts the compressive strength of the samples. The pozzolanic activity is evident in S1 as the strength activity index increased from 76.5% to 87.9% for 7d and 28d curing, respectively. However, the 7d strength activity index at 50% replacement was 42%, out of the ASTM C618 standard limit (≥75%). Although the strength index increased to almost 72.8% upon curing for 28d, the value is still unacceptable. This is mainly attributed to the deficiency of the portlandite $Ca(OH)_2$ at a high fraction of WG. Previous studies reported a poor pozzolanic reaction, especially when the replacement fraction of WG with cement in concrete exceeded 30%. Excessive dilution of cement with WG (beyond 30%) caused a substantial decrease in the compressive strength of concrete due to the portlandite lack, a key factor in the pozzolanic reaction [40].

In the same context, the strength activity indices of SS (S3) were 47% and 48.7% for 7 d and 28 d curing, respectively. These suggest SS failed to replace cement even though cementitious materials (C_3S and C_2S) are presented in SS composition, see Figure 6. The strength index indicates that SS chemistry is not the exclusive criterion for hydraulic activity evaluation. Indeed, two physical factors named the temperature of the formation and cooling rate of the SS are also crucial [41]. As discussed in the introduction, these factors may dramatically deteriorate SS hydraulic activity. Moreover, the strength index of S2 was much higher than that of S3 (both at 50% replacement for cement), justifying the cementitious capability of WG compared with SS.

Nevertheless, the weak slag activity does not prevent replacing SS with aggregates. In contrast, cementitious compounds may add beneficial potentials to SS over natural aggregates. The cementitious materials may lead to a compacted interfacial transition zone (ITZ) near SS aggregates, improving the mechanical properties of mortar and concrete [42].

Table 6: Results of the flow table test

Samples	Water to binder ratio (w/b)	Flow of mortars (%)
S_0	0.775	106
S_1	0.725	109
S_2	0.725	114
S_3	0.800	112

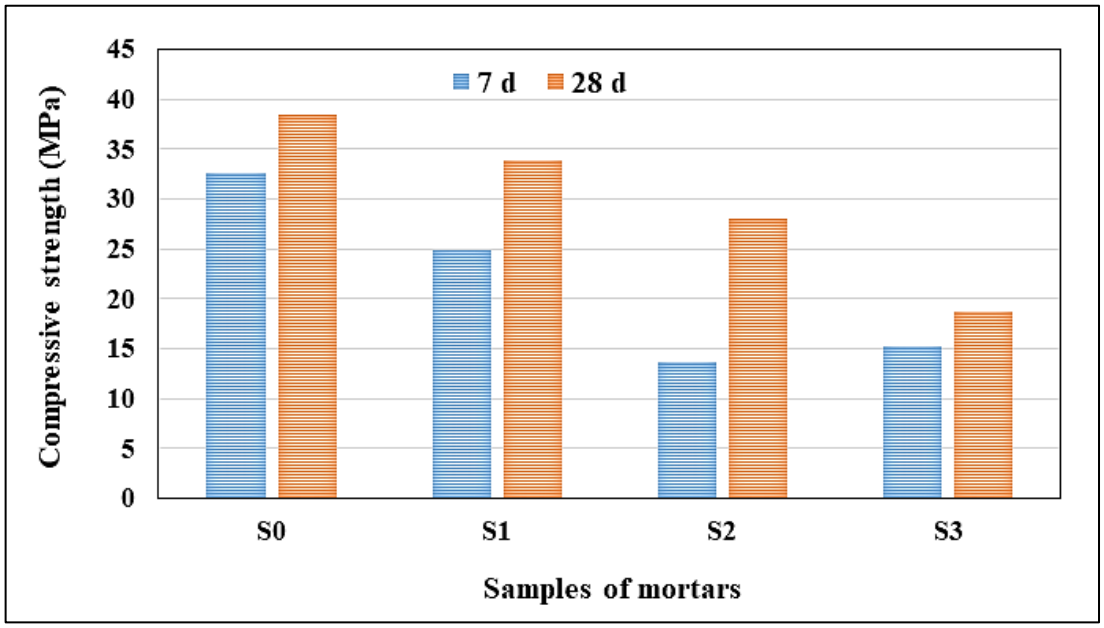

Figure 8: Effect of SS and WG on the compressive strength of mortars

3.5 Steel Slag as Coarse Aggregates in Concrete

3.5.1 Workability of Concrete

The workability results are shown in Figure 9. The slump of all samples was within the target range upon incorporation of 0.5% weight percent SP as a ratio of binder (cement+ WG). However, the slump increased from 205 mm to 210 mm upon incorporation of 15%WG at 0% SS. The positive effect of WG on workability has already been discussed in the previous sections. On the other hand, the slump decreased to 185 mm and 170 mm when 50% SS replaced CA in A2 and A3, respectively, owing to the friction exerted on the paste by SS. A higher slump decrease in A3 with no WG than A2 confirms WG and SS's positive and negative influence on workability, respectively. The negative impact of SS on the workability is mainly attributed to its irregular texture and porous nature, which may absorb water, reducing the workability see Figure 1.

3.5.2 Compressive strength of concrete

The results of the compressive strength for 28d and 91d curing, abbreviated here as fc28 and fc91, respectively, are shown in Figure 10. Both fc28 and fc91 decreased in A1 by about 18.4% and 7.8% respectively when compared with A0. The incorporation of 15% WG might decrease the compressive strength. The low compressive strength of A1 with 15% WG versus A3 (no WG) also confirms the detrimental influence of WG. However, incorporating SS into concrete may compensate for the WG's negative actions. In this regard, both fc28 and fc91 increased about 18.7% and 14.4%, respectively, in A2 on that of A1 when 50% SS was added to concrete with already 15% WG. This improvement in the compressive strength supports the assumption of SS efficiency in reducing the negative impacts of WG. A similar behavior was reported in the literature where the compressive strength increased dramatically when SS increased at a constant value of WG owing to its high hardness [43]. Nevertheless, the maximum fc91 was at A3, with more than 10% improvement compared with the control sample (A0).

Notably, the maximum improvement in fc91 was in A3 (65.51MPa), corresponding to an increase of about 11% and 20% on A0 and A1, respectively. This is an additional justification for SS's positive role in concrete compressive strength. A proper explanation for the SS mechanical performance in concrete might be its irregular texture see Figure 1 and/or the delayed hydration of its cementitious materials see Figure 4. These both motivate intimate contact with paste, enhancing the microstructural integrity of the interfacial transition zone (ITZ) near SS. A similar justification was reported in the literature when Wu et al. analyzed the microstructure of ITZ using backscattered electron images. It was noted that the SS/paste interface was compacted and had fewer micro-cracks than the CA/paste interface because of SS's rough surface and hydration activity [42].

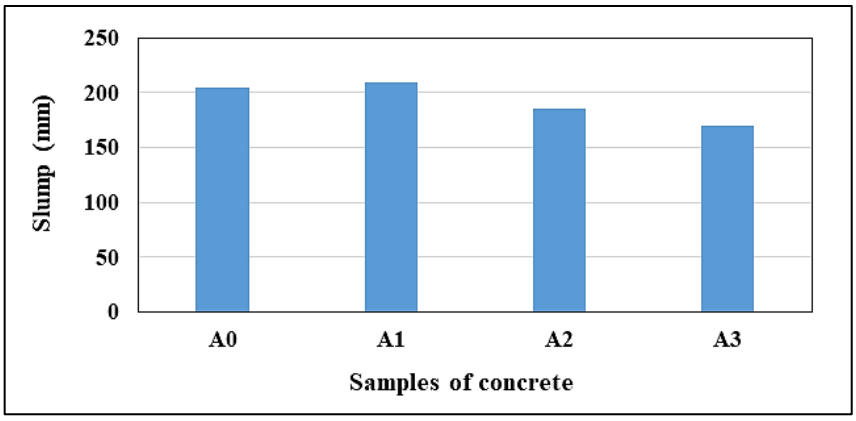

Figure 9: Effects of SS and WG on the concrete workability

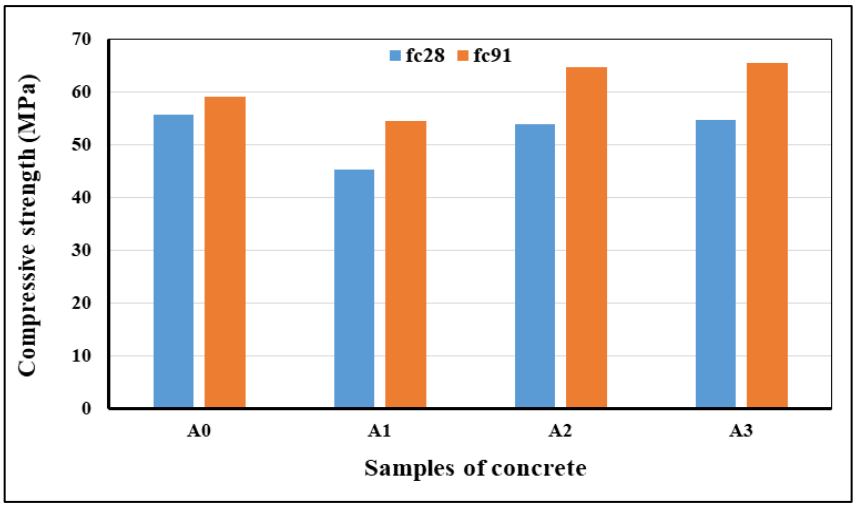

Figure 10: Effects of SS and WG on fc28 and fc91 of concrete

3.5.3 Scanning electron microscope

Figure 11. depicts the results of SEM of concrete in which the microstructure of ITZ near SS (A2) was evaluated against the control sample (A0). The images completely confirm the structural integrity at the SS/ Paste interface owing to filling with the hydration products see Figure 11a. The irregular texture of SS cohesively interfered with the paste, causing a substantial reduction in the porosities' numbers and the width of micro-cracks at ITZ in contrast to that at CA Figure 11b.

The cementitious capability of the SS, despite its weakness in replacing cement, might have significantly influenced the synergistic bonding between SS aggregates and paste. Penetration of the paste deep inside into the porosities of SS might be another reason for dense ITZ near the SS surface [44]. Moreover, retained water in these porosities might cause delayed hydration at the SS surface. Costa et al. also reported this justification when they observed the porosity on the surface of the SS aggregates. The significant improvement in the mechanical properties of the concrete in their research was attributed to the porous nature of SS [45]. The findings of the SEM analysis of this study provide further evidence for the positive impact of using steel slag as an aggregate in concrete. The delayed hydration in the SS porosities is responsible for the dense and compacted ITZ near SS aggregates and the overall improved mechanical properties of concrete upon incorporation of SS, as discussed in the previous section.

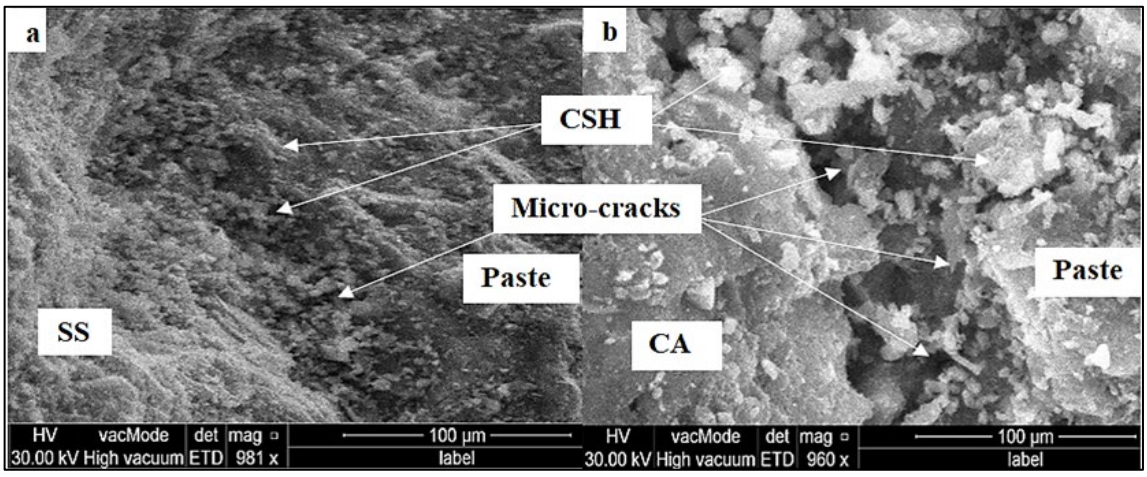

Figure 11: SEM analysis of ITZ at a) SS/Paste interface and b) CA/ paste interface

4. Conclusion

This study attempted to replace SS and WG with cement to produce a green construction material. The corresponding outputs would have various ecological benefits such as removing SS and WG from the landscapes, resulting in a cleaner environment. However, the basic conclusions drawn from the experiments are as follows:

1) SS cannot replace cement due to its poor pozzolanic activity, unlike WG, which met the pozzolan materials criteria and can replace cement successfully. This probably suggests SS as a CA replacement.
2) SS negatively affects the workability of both mortar and concrete owing to its irregular shape in contrast to WG which improved the workability because of its hydrophobic nature.
3) In mortars, the density increased with SS and decreased with WG when both replaced cement. Their intrinsic specific gravity, which is high for SS and low for WG compared with cement, may justify the trend of the density variation in mortars.
4) The irregular texture of SS derives its positive influence on the compressive strength of concrete. In addition to that, SS also compensated for the reduction of concrete's compressive strength due to WG incorporation.

Author contributions

Conceptualization, A. Azeez, M. Hassan and A. Attiyah.; formal analysis, A. Azeez, M. Hassan; investigation, A. Azeez; data curation, A. Azeez; writing—original draft preparation, A. Azeeza, M. Hassan, and A. Attiyah; writing—review and editing, A. Azeeza, M. Hassan, and A. Attiyah. All authors have read and agreed to the published version of the manuscript.

Funding

This research received no external funding.

Data availability statement

The data that support the findings of this study are available on request from the corresponding author.

Conflicts of interest

Not applicable.

References

[1] A. Maries, C.D. Hills, P. Carey, Low-Carbon CO_2-Activated Self-Pulverizing Cement for Sustainable Concrete Construction, J. Mater. Civ. Eng., 32 (2020) 1–5. https://doi.org/10.1061/(ASCE)MT.1943-5533.0003370

[2] K. K. Aswed, M.S. Hassan, H. Al-quraishi, Optimisation and Prediction of Fresh Ultra-High-Performance Concrete Properties Enhanced with Nanosilica, Adv. Concr. Technol., 20 (2022) 103–116. https://doi.org/10.3151/jact.20.103

[3] I. K. Harith, M.S. Hassan, S.S. Hasan, Liquid nitrogen effect on the fresh concrete properties in hot weathering concrete, Innov. Infrastruct. Solut., 7 (2022). https://doi.org/10.1007/s41062-021-00731-6

[4] H. Yi, G. Xu, H. Cheng, J. Wang, Y. Wan, H. Chen, An Overview of Utilization of Steel Slag, Procedia Environ. Sci., 16 (2012) 791–801. https://doi.org/10.1016/j.proenv.2012.10.108

[5] H. Hamada, A. Alattar, B. Tayeh, F. Yahaya, B. Thomas, Effect of recycled waste glass on the properties of high-performance concrete: A critical review, Case Stud. Constr. Mater., 17 (2022) e01149. https://doi.org/10.1016/j.cscm.2022.e01149

[6] Z. Abed, H. Ahmed, W. Khalil, Optimization of Silica Fume and Slag in Roller Compacted Concrete by Taguchi Method, Eng. Technol. J., 41 (2023) 724–733. https://doi.org/10.30684/etj.2023.138600.1411

[7] C. S. Ezenkwa, T.I. Elogu, Uncracked Palm Kernel Shell Effect on Compressive Strength of Concrete, Eng. Technol. J. 41 (2023) 1–8. http://doi.org/10.30684/etj.2023.140014.1460

[8] C. Thomas, J. Rosales, J.A. Polanco, F. Agrela, Steel slags, Elsevier Ltd, 2018. https://doi.org/10.1016/B978-0-08-102480-5.00007-5

[9] H. Alanyali, M. Çöl, M. Yilmaz, Ş. Karagöz, Concrete produced by steel-making slag (basic oxygen furnace) addition in portland cement, Int. J. Appl. Ceram. Technol., 6 (2009) 736–748. https://doi.org/10.1111/j.1744-7402.2008.02317.x

[10] N.Y. Mostafa, S.A.S. El-Hemaly, E.I. Al-Wakeel, S.A. El-Korashy, P.W. Brown, Characterization and evaluation of the hydraulic activity of water-cooled slag and air-cooled slag, Cem. Concr. Res., 31 (2001) 899–904. https://doi.org/10.1016/S0008-8846(01)00497-5

[11] A.M. Rashad, A synopsis manual about recycling steel slag as a cementitious material, J. Mater. Res. Technol., 8 (2019) 4940–4955. https://doi.org/10.1016/j.jmrt.2019.06.038

[12] E.T. Dawood, M.S. Mhmood, Properties of binary blended cement mortars containing glass powder and steel slag powder, Eng. Trans., 69 (2021) 243–256. https://doi.org/10.24423/EngTrans.1266.20210802

[13] O. Gencel, O. Karadag, O.H. Oren, T. Bilir, Steel slag and its applications in cement and concrete technology: A review, Constr. Build. Mater., 283 (2021) 122783. https://doi.org/10.1016/j.conbuildmat.2021.122783

[14] I. Kattoof, M.S. Hassan, S.S. Hasan, Effects of Liquid Nitrogen Cooling on the Microstructure Properties of Nano - Modified Concrete Under Hot Conditions, Arab. J. Sci. Eng., (2022). https://doi.org/10.1007/s13369-021-06496-5

[15] B. Omer, J. Saeed, Effect of water to binder ratio and particle size distribution of waste glass powder on the compressive-strength and modulus of elasticity of normal-strength concrete, Eur. J. Environ. Civ. Eng., 26 (2022) 5300–5321. https://doi.org/10.1080/19648189.2021.1893227

[16] S.K. Kim, I.Y. Jang, H.J. Yang, Strength Development Characteristics of Concrete Replaced with Different Waste Glasses from Display Industry as a Cementitious Material, KSCE J. Civ. Eng., 24 (2020) 2485–2494. https://doi.org/10.1007/s12205-020-0223-y

[17] S. Abdulmunem, S. Hasan, Effect of Glass Wastes on Basic Characteristics of Controlled Low-Strength Materials, Eng. Technol. J., 40 (2022) 1455–1464. https://doi.org/10.30684/etj.2022.132930.1155

[18] N. Almesfer, J. Ingham, Effect of Waste Glass on the Properties of Concrete, J. Mater. Civ. Eng., 26 (2014) 1–6. https://doi.org/10.1061/(asce)mt.1943-5533.0001077

[19] ASTM C 150/ C150M, Standard specification for portland cement, ASTM International, West Conshohocken, PA, 2019., n.d. https://doi.org/10.1520/C0150

[20] ASTM C618, Standard Specification for Coal Fly Ash and Raw or Calcined Natural Pozzolan for Use in Concrete, ASTM International, West Conshohocken, PA, 2015, n.d. https://doi.org/10.1520/C0618-19.2

[21] ASTM Standard C128, Standard Test Method for Density, Relative Density (Specific Gravity), and Absorption of Fine Aggregate, ASTM International, West Conshohocken, PA, 2007., n.d.

[22] ASTM Standard C989, Standard Specification for Ground Granulated Blast-Furnace Slag for Use in Concrete and Mortars, ASTM International, West Conshoocken, PA, 2005. www.astm.org.

[23] ASTM Standard C127, Standard Test Method for Density , Relative Density (Specific Gravity), and Absorption of Coarse Aggregate, ASTM International, West Conshohocken, PA, 2007, n.d.

[24] ASTM Standard C305, Standard Practice for Mechanical Mixing of Hydraulic Cement Pastes and Mortars, ASTM International, West Conshohocken, PA, 1999.

[25] ASTM Standard C109/109M, Standard Test Method for Compressive Strength of Hydraulic Cement Mortars, ASTM International, West Conshohocken, PA, 2020.

[26] ASTM C642, Standard Test Method for Density, Absorption, and Voids in Hardened Concrete, ASTM International, West Conshohocken, PA. 2006., n.d.

[27] ASTM C1437,Standard Test Method for Flow of Hydraulic Cement Mortar, ASTM International, West Conshohocken, PA, 2007, n.d.

[28] K. Aswed, M. Hassan, H. Al-Quraishi, Effects of Curing Temperature and Chemical Admixture Type on Fresh Properties and Compressive Strength of Ultra High-performance Concrete, Eng. Technol. J., 40 (2022) 1448–1454. https://doi.org/10.30684/etj.2022.132300.1103

[29] ASTM C778, Standard Specification for Standard Sand, ASTM International , West Conshohocken, PA, 2002., n.d.

[30] M. Zhou, X. Cheng, X. Chen, Studies on the volumetric stability and mechanical properties of cement-fly-ash-stabilized steel slag, Materials (Basel). 14 (2021) 1–16. https://doi.org/10.3390/ma14030495

[31] ACI Committee 211. Standard practice for Selecting Proportions for Normal, Heavyweight, and Mass Concrete: (ACI 211.1-91). American Concrete Institute, 1991., n.d.

[32] ASTM Standard C192/192M, Standard Practice for The, Making and Curing Concrete Test Specimens in Laboratory, ASTM International, West Conshohocken, PA, 2002., n.d.

[33] ASTM Standard C143/143M, Standard Test Method for Slump of Hydraulic-Cement Concrete, ASTM International, West Conshohocken, PA, 2010.

[34] ASTM C 39/C 39M. Standard Test Method for Compressive Strength of Cylindrical Concrete Specimens, ASTM International, West Conshohocken, PA, 2014., n.d. https://doi.org/10.1520/C0039

[35] K. Liu, Z. Zhang, J. Sun, Advances in Understanding the Alkali-Activated Metallurgical Slag, Adv. Civ. Eng., 2021 (2021). https://doi.org/10.1155/2021/8795588

[36] B. Omer, J. Saeed, Long-Term Effect Of Different Particle Size Distributions Of Waste Glass Powder On The Mechanical Properties, (2020) 61–75. https://doi.org/10.21307/ACEE-2020-030

[37] X. Zhuang, Y. Liang, J.C.M. Ho, Y.H. Wang, M. Lai, X. Li, Z. Xu, Y. Xu, Post-fire behavior of steel slag fine aggregate concrete, Struct. Concr., 23 (2022) 3672–3695. https://doi.org/10.1002/suco.202100677

[38] J. Abellán, J. Fernández, N. Torres, A. Núñez, Statistical optimization of ultra-high-performance glass concrete, ACI Mater. J., 117 (2020) 243–254. https://doi.org/10.14359/51720292

[39] A. Siddika, A. Hajimohammadi, W. Ferdous, V. Sahajwalla, Roles of waste glass and the effect of process parameters on the properties of sustainable cement and geopolymer concrete—a state-of-the-art review, Polymers (Basel). 13 (2021). https://doi.org/10.3390/polym13223935

[40] H. Du, K.H. Tan, Waste glass powder as cement replacement in concrete, J. Adv. Concr. Technol., 12 (2014) 468–477. https://doi.org/10.3151/jact.12.468

[41] G. Sheng, C. Li, S. Jin, Q. Bai, Effects of Steel Slag Powder as A Cementitious Material on, (2023).

[42] K. Wu, J. Han, Quantitative evaluation of interfacial transition zone of sustainable concrete with recycled and steel slag as aggregate, Structural Concrete, 22 (2021) 926–938. https://doi.org/10.1002/suco.202000135

[43] S. Rehman, S. Iqbal, A. Ali, Combined influence of glass powder and granular steel slag on fresh and mechanical properties of self-compacting concrete, Constr. Build. Mater., 178 (2018) 153–160. https://doi.org/10.1016/j.conbuildmat.2018.05.148

[44] R. Chen, K.H. Mo, T.C. Ling, Offsetting strength loss in concrete via ITZ enhancement: From the perspective of utilizing new alternative aggregate, Cem. Concr. Compos., 127 (2022). https://doi.org/10.1016/j.cemconcomp.2021.104385

[45] L.C.B. Costa, M.A. Nogueira, H.D. Andrade, J.M.F. de Carvalho, F.P. da F. Elói, G.J. Brigolini, R.A.F. Peixoto, Mechanical and durability performance of concretes produced with steel slag aggregate and mineral admixtures, Constr. Build. Mater., 318 (2022). https://doi.org/10.1016/j.conbuildmat.2021.126152